http://dx.doi.org/10.5012/bkcs.2012.33.2.541

Solution Processable Symmetric 4-Alkylethynylbenzene End-Capped Anthracene Derivatives

Sang Hun Jang, Hyunjin Kim, Min Ji Hwang, Eun Bin Jeong, Hui Jun Yun,[†] Dong Hoon Lee,[‡] Yun-Hi Kim, Chan Eon Park,[‡] Yong-Jin Yoon, Soon-Ki Kwon,[†,*] and Sang-Gyeong Lee[*]

Department of Chemistry, Graduate School for Molecular Materials and Nanochemistry, Gyeongsang National University, Jinju 660-701, Korea. [*]E-mail: leesang@gnu.ac.kr
[†]School of Nano & Materials and Engineering Research Institute, Gyeongsang National University, Jinju 660-701, Korea
[‡]Polymer Research Institute, Department of Chemical Engineering, Pohang University of Science and Technology, Pohang 790-784, Korea
Received November 3, 2011, Accepted December 9, 2011

New candidates composed of anthracene and 4-alkylethynylbenzene end-capped oligomers for OTFTs were synthesized under Sonogashira coupling reaction conditions. All oligomers were characterized by FT-IR, mass, UV-visible, and PL emission spectrum analyses, cyclic voltammetry (CV), differential scanning calorimetry (DSC), thermal gravimetric analysis (TGA), ^{1}H-NMR, and ^{13}C-NMR. Investigation of their physical properties showed that the oligomers had high oxidation potential and thermal stability. Thin films of **DHPEAnt** and **DDPEAnt** were characterized by spin coating them onto Si/SiO_2 to fabricate top-contact OTFTs. The devices prepared using **DHPEAnt** and **DDPEAnt** showed hole field-effect mobilities of 4.0×10^{-3} cm^2/Vs and 2.0×10^{-3} cm^2/Vs, respectively, for solution-processed OTFTs.

Key Words : Solution-processing, Anthracene derivatives, Sonogashira coupling, Organic thin-film transistors

Introduction

Organic field-effect transistors (OFETs) have attracted much attention because of their potential applications to low-cost electronic devices and their integrated circuits.[1] These applications tend to focus on macroelectronics in the arenas of large area displays, electronic bar codes and identification tags, and flexible electronics such as wearable sensors and electronic paper.[2] Hole mobilities in anthracene single crystals were measured by the time-of-flight photocurrent technique and found to reach up to 3 $cm^2V^{-1}s^{-1}$ at 300 K.[3] Although anthracene may be a good candidate for a p-type semiconductor for OFETs, FET activity has not yet been observed.[4] The HOMO energy level in linear [*n*]acenes (*n* = 2: naphthalene, 3: anthracene, 4: tetracene, 5: pentacene) significantly increases with increasing *n*, which facilitates the formation of radical cations (holes) at the interface between a dielectric and a semiconducting layer. Furthermore, the extended π system of a higher acene enhances the intermolecular overlap of π-π systems in the solid state and leads to high mobility. However, a problem of the linear acene approach is the chemical instability of higher acenes.[5,6] Recent developments by several groups have led to improved stability, primarily through the judicious choice of conjugated units and side chains.[7,8] Meng's group reported a new organic semiconductor, which had an asymmetrically substituted phenylenevinyleneanthracene backbone pendant with pentyl groups as side chains. The molecule's crystal packing is denser than that of pentacene. Devices incorporating this semiconductor show a remarkably high charge carrier mobility of 1.28 cm^2/Vs, environmental stability, and device repeatability. These anthracene derivatives were introduced with a phenylenevinylene moiety for increased mobility. In addition, introducing a pentyl side chain to phenylenevinyleneanthracene leads to a good molecular ordering of the alkyl side chain, especially at high substrate temperatures.[9]

Kwon's group in particular has demonstrated a high mobility anthracene/naphthalene hybrid semiconductor. They reported alkoxylnaphthyl-end-capped oligomers (ANANE) displaying stable device performance with a mobility of up to 0.20 cm^2/Vs. The material also showed high oxidative and thermal stability.[10]

Thus, pentacene and fused aromatic materials have been extensively studied for use in OTFTs because of their relatively high mobilities. However, it is difficult to fabricate OTFTs by using solution-process because pentacene and fused aromatic materials have significantly low solubility in common organic solvents.

Therefore, we envision that the phenyl function will show a more extended π-conjugation length. The oxidative stability of arylethynyl-substituted anthracene may be improved by the introduction of ethynyl functions. Introduction of a long alkyl side chain will increase solubility and molecular ordering. Thus, we modified the anthracene molecule by introducing acetylene to increase oxidative stability or by introducing a long decyl end group to increase solubility and fine molecular ordering due to improved self-assembly properties.[11,12]

In this paper, we report the synthesis and characteristics of

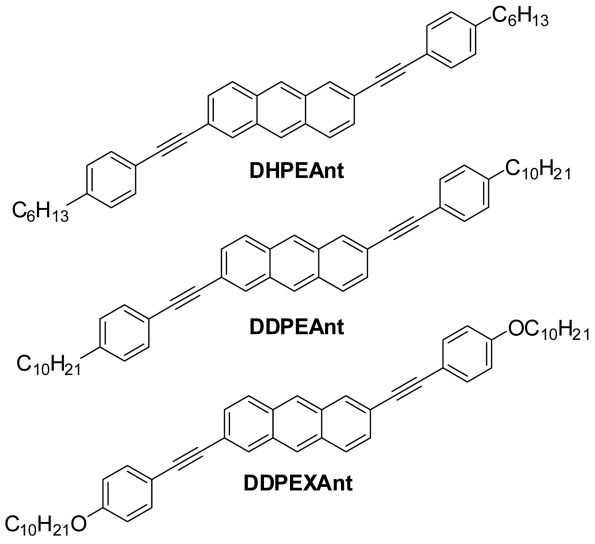

Scheme 1. Structures of **DHPEAnt**, **DDPEAnt**, and **DDPEXAnt**.

novel anthracene derivatives for OTFTs, composed of anthracene as a core unit and 4-alkylethynylbenzene as the end-capper. In addition, we report the electrochemical properties and TFT characteristics of the synthesized molecules.

Results and Discussion

Synthesis and Characterization. The synthetic strategy to obtain the desired molecules is illustrated in Schemes 2 and 3. Compounds **5a-c** were prepared from bromobenzene and 4-bromophenol as starting materials (Scheme 2). The acylated compounds **1a-b** were readily obtained by Friedel-Crafts acylation with aluminium chloride, decanoyl chloride, and bromobenzene. Compounds **1a-b** were reduced by the Wolff-Kishner reaction in the presence of hydrazine hydrate, KOH, and triethylene glycol to give compounds **2a-b** in 48% and 59% yield, respectively. 4-Bromophenol was esterified with 1-bromodecane in the presence of NaI, KOH, and ethanol to give compound **3** in 98% yield. 4-Bromoalkylbenzenes (**2a-b** and **3**) were added to the appropriate trimethylsilylacetylene by the Sonogashira coupling reaction in the presence of a palladium catalyst. The resulting products **3a-c** were then desilylated. It should be noted that (2-(4-alkylphenyl)ethynyl)trimethylsilanes were easily desilylated under normal desilylation conditions, for example, with tetrabutylammonium fluoride in tetrahydrofuran. 2,6-Dibromoanthracene was synthesized according to procedures in the literature.[13]

The obtained **5a-c** were used for a coupling reaction with 2,6-dibromoanthracene in the next step. The target material **DHPEAnt**, **DDPEAnt** and **DDPEXAnt** were synthesized under the conditions of Sonogashira coupling reactions in the presence of a palladium catalyst in diisopropylamine: toluene (1:1) to give 50%, 38% and 27% yield, respectively (Scheme 3). **DHPEAnt**, **DDPEAnt** and **DDPEXAnt** were soluble in common solvents such as chloroform, toluene, chlorobenzene, and so on. Therefore, their structures were

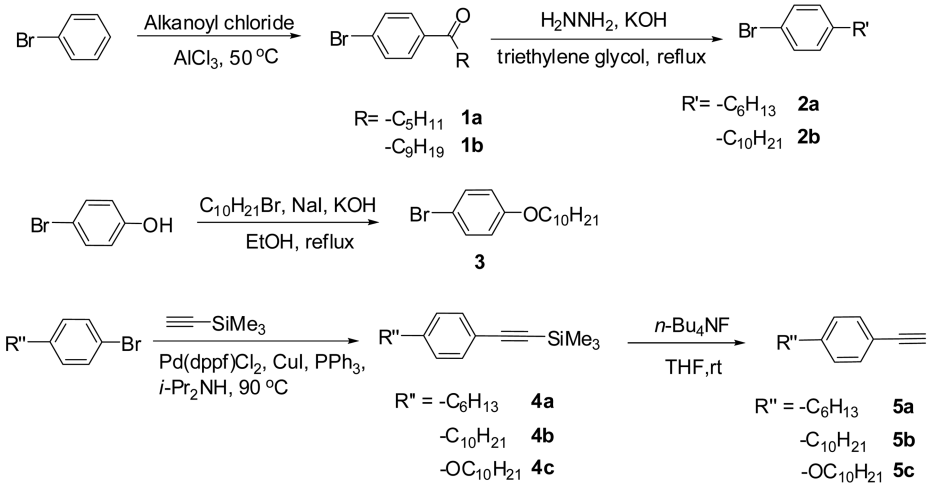

Scheme 2. Synthetic methods for the preparation of 1-ethynyl-4-alkylbenzenes **5a**-**5c**.

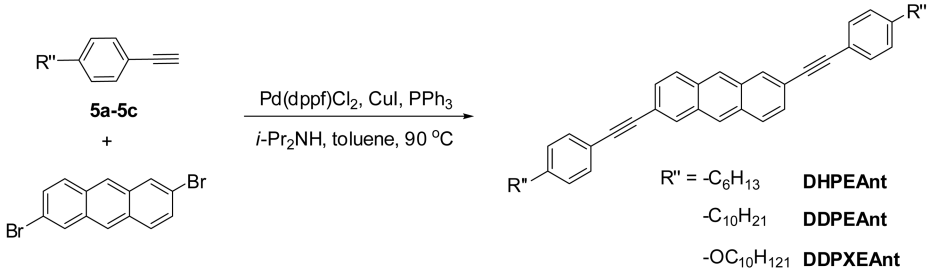

Scheme 3. Synthesis of **DHPEAnt**, **DDPEAnt**, and **DDPEXAnt**.

Table 1. UV-visible and PL spectra of **DHPEAnt**, **DDPEAnt**, and **DDPEXAnt**

Compound	$\lambda_{abs/nm}$ [a]		$\lambda_{em/nm}$ [b]	
	Solution	Film	Solution	Film
DHPEAnt	393, 417	405, 438	429, 452	477
DDPEAnt	392, 415	410, 438	426, 450	479, 510
DDPEXAnt	390, 412	393, 415, 442	424, 448	483, 516

[a]Measured in dilute $CHCl_3$ solution and thin film state. [b]Excited at the absorption maxima

confirmed by FT-IR, ^{1}H-NMR, ^{13}C-NMR, and mass analysis.

Optical Properties. The optical properties of synthesized oligomers were investigated using UV-vis absorption and photoluminescence (PL) in a dilute $CHCl_3$ solution and on thin films. The results are shown in Figure 1 and 2. The oligomer films were prepared on quartz substrates by dip-coating from the chloroform solutions at room temperature. UV-vis absorption and PL emission spectral datas of the oligomers are given in Table 1. Thin films of **DHPEAnt**, **DDPEAnt** and **DDPEXAnt** show a red shift of the main absorption peak compared to that obtained in dilute chloroform solution. This red shift is typically indicative of favourable interactions and stacking between the molecules in the solid state, which leads to greater electron delocalization.[14] In terms of PL spectra, the oligomers exhibited blue fluorescence in solution. The emission spectra of oligomers in the solid state displayed a large red shift of about 30-50 nm. These results may originate from the formation of aggregations or excimers in the thin film due to π-π stacking or to intermolecular interactions caused by their planar structure. [15]

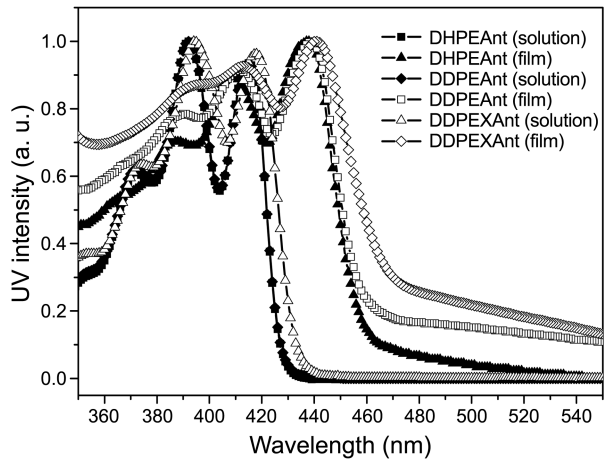

Figure 1. UV-vis absorption of **DHPEAnt**, **DDPEAnt**, and **DDPEXAnt** in dilute $CHCl_3$ solution and in the solid state.

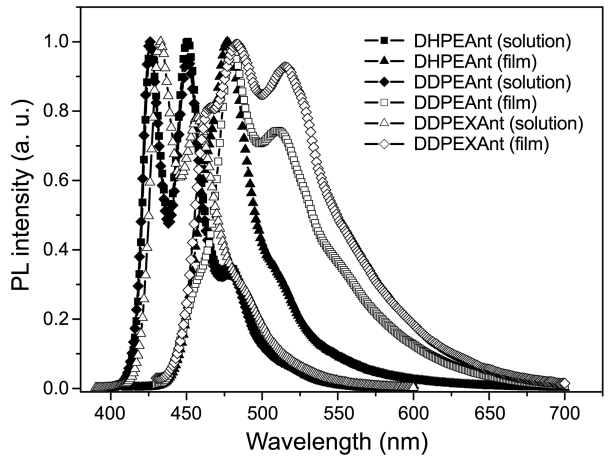

Figure 2. Photoluminescence spectra of **DHPEAnt**, **DDPEAnt**, and **DDPEXAnt** in dilute $CHCl_3$ solution and in the solid state.

DDPEXAnt showed a greater red shift than **DDPEAnt** in the film state because of improved π-π intermolecular interactions due to the introduction of the end-capping electron donor alkoxybenzene.

Electrochemical Properties. The electrochemical behaviors of oligomers were investigated by cyclic voltammetry (CV). The cyclic voltammograms (CV) of the oligomers were recorded in a 1.0×10^{-3} M $CHCl_3$ solution containing 0.1 M Bu_4NClO_4. The oxidation peak potentials of oligomers are summarized in Table 2. In addition, the optical band gaps (E_g) of the anthracene derivatives were determined from absorption onset and found to be 2.90, 2.88 and 2.85 eV for **DHPEAnt**, **DDPEAnt** and **DDPEXAnt**, respectively. Table 2 also summarizes the HOMO/LUMO energies of **DHPEAnt**, **DDPEAnt** and **DDPEXAnt** estimated from the relation $E_{(LUMO)} = E_{(HOMO)} + E_{gap}$, where $E_{(HOMO)}$ is classically estimated from E_{onset} [x].[16] The HOMO energy levels of anthracene derivatives were shown to be in the range of −5.38 to −5.43 eV. The bandgaps and HOMO levels of the obtained oligomers are larger and lower, respectively, than those of pentacene (HOMO level of −5.0 eV). This reveals that, due to their alkyl and alkoxy linkages, the oligomers have a higher electron density and more effective conjugation ability. As a result, their oxidation potential is lower than that of pentacene.

For p-type semiconductors, the majority carriers are holes. For this reason, it is important to reduce the energy barrier between the gold electrode and the organic semiconductor so that the HOMO levels of p-type semiconductors is close to the work function of the gold electrode (−5.4 eV).[17] Therefore, it can be assumed that the injection of charge carriers may be hindered. In addition, the determined HOMO levels of p-type semiconductors match well with the work function of the gold metal used in OTFTs, which leads to increased efficiency of hole injection and transport.

Table 2. Electrochemical properties of **DHPEAnt**, **DDPEAnt**, and **DDPEXAnt**

Compound	Oxidation E_{onset} (V)	HOMO/eV	LUMO/eV	Eg/eV
DHPEAnt	0.87	-5.39	-2.41	2.98
DDPEAnt	0.88	-5.38	-2.44	2.94
DDPEXAnt	0.91	-5.43	-2.50	2.93

※ HOMO-LUMO gap measured according to the onset of UV absorption (=1240/λ_{onset} eV). HOMO (eV) measured according to the onset of oxidation (HOMO = 4.44+E_{onset}; ferrocene = 4.84-E_{onset} (oxidation of ferrocene) = 4.84−0.40 = 4.44).

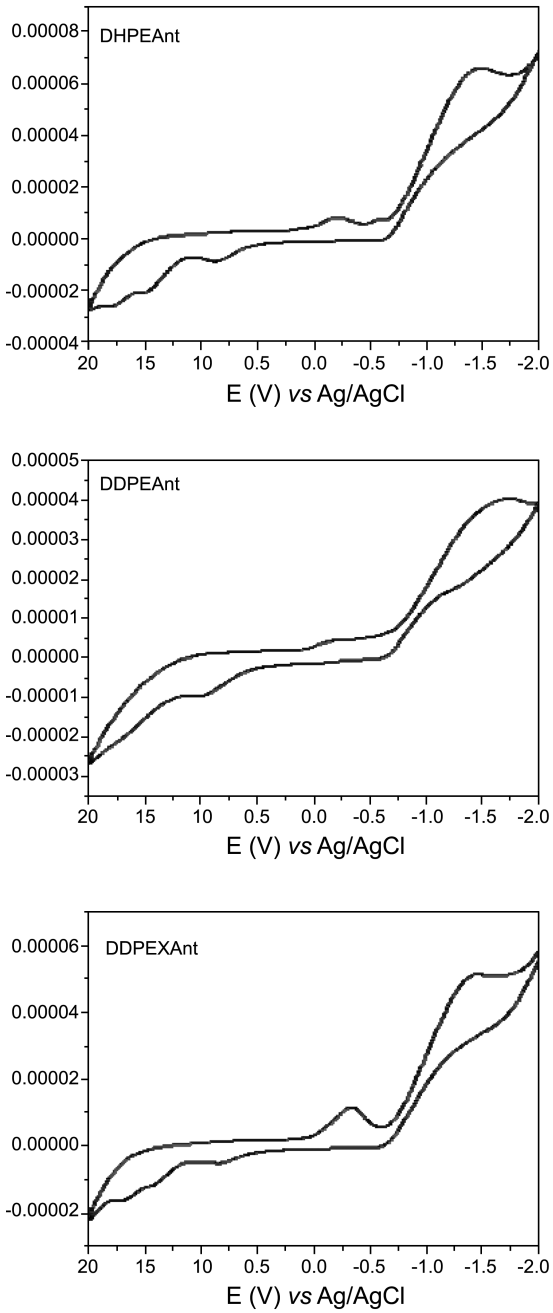

Figure 3. Cyclic voltammograms of **DHPEAnt**, **DDPEAnt**, and **DDPEXAnt** in 0.1 M Bu_4NClO_4 at a scan rate of 50 mV/s.

Thermal Properties. Thermal gravimetric analysis (TGA) reveals that **DHPEAnt**, **DDPEAnt** and **DDPEXAnt** have high thermal stability with decomposition temperatures (T_d) of 438, 453 and 417 °C, respectively, under a nitrogen atmosphere. The results are shown in Figure 3. Differential scanning calorimetry (DSC) gives the major endothermic melting peaks for **DHPEAnt**, **DDPEAnt** and **DDPEXAnt** as 217, 199 and 226 °C, respectively and the corresponding major exothermic crystallization peaks as 211, 194 and 220 °C, respectively. DSC reveals reversible melting features for anthracene derivatives with each material exhibiting two thermal transitions before melting. Figure 4 illustrates the heating and cooling process for **DHPEAnt**, **DDPEAnt** and

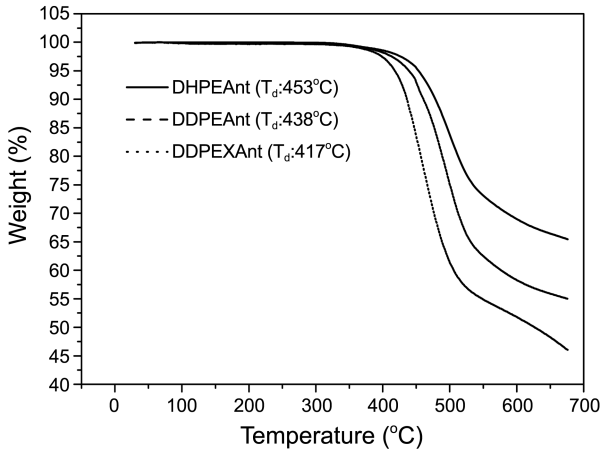

Figure 4. TGA curves of **DHPEAnt**, **DDPEAnt**, and **DDPEXAnt**.

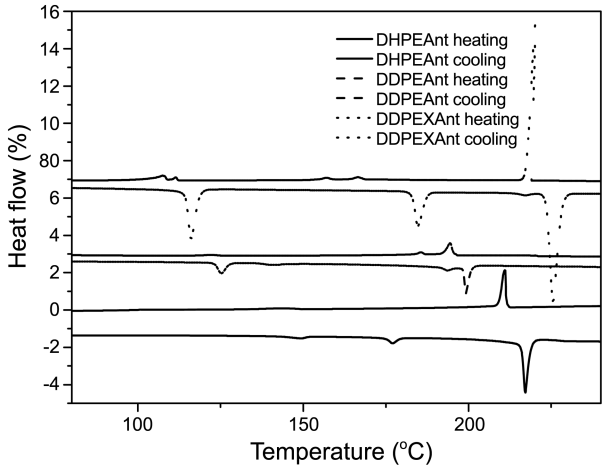

Figure 5. DSC thermograms of **DHPEAnt**, **DDPEAnt**, and **DDPEXAnt**.

DDPEXAnt. The thermal features of **DHPEAnt**, **DDPEAnt** and **DDPEXAnt** show that all three oligomers are crystalline. Therefore, it is expected that their thin films are well-ordered under heat treatment.

OTFT Characterization. The semiconducting properties of the anthracene derivatives were investigated by fabricating OTFT devices in top-contact configuration. For preliminary transistor measurements, the active layers of the anthracene derivatives were spin-coated from 0.5 wt % chloroform solutions without further thermal treatment. TFT device characteristics cooperating with **DHPEAnt** and **DDPEAnt** are summarized in Table 3. Figure 5 shows a plot of the drain current (I_d) versus gate voltage (V_g) along with a plot of the drain current (I_d) versus drain-source voltage (V_d) for a **DHPEAnt**-based OTFT showing the highest performance in terms of both mobility (4.0×10^3 cm^2/Vs) and on/off ratio (10^5). In the case of **DHPEAnt**, the relatively shorter alkyl chain may produce a more crystalline structure than in the case of **DDPEAnt**. The thermally stable **DHPEAnt** also shows an increased field effect mobility of 4.0×10^{-3} cm^2/Vs after a 160 °C thermal annealing process. With further annealing above 180 °C, a temperature higher

Table 3. TFT properties of **DHPEAnt** and **DDPEAnt**

Compound	Annealing temperature (°C)	Mobility[a]	On/off ratio[a]	Threshold voltage[a]
DHPEAnt	RT	0.002 cm^2/Vs	3×10^5	-11.5 V
	160	0.004 cm^2/Vs	10^5	-11.3 V
	180	0.001 cm^2/Vs	10^5	-7.0 V
DDPEAnt	RT	-	-	-
	160	0.002 cm^2/Vs	2×10^4	-4.2 V
	180	-	-	-

[a]Top-contact, OTS, spin-coating

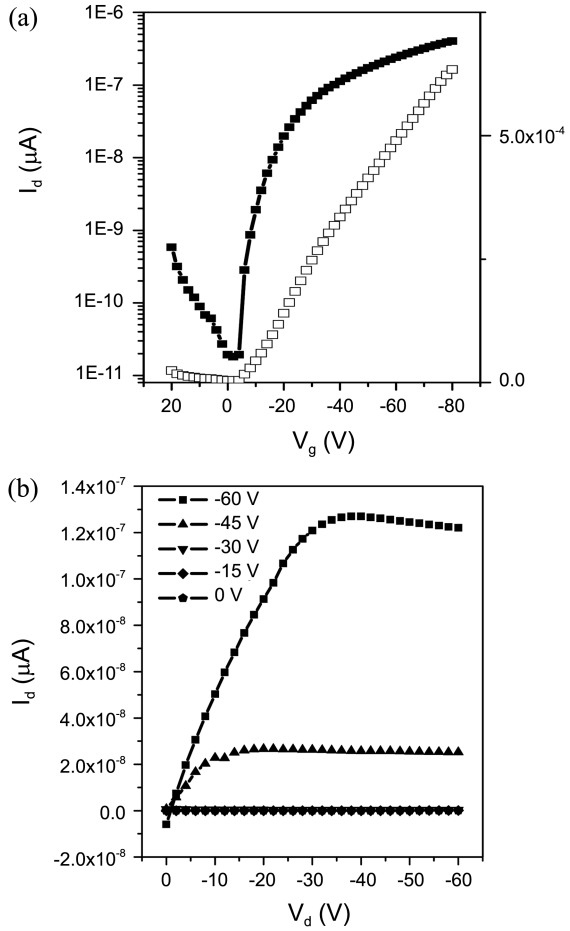

Figure 6. (a) Drain current (I_d) versus gate voltage (V_g) characteristics of **DDPEAnt**. (b) Drain current (I_d) versus drain-source voltage (V_d) characteristics of the **DDPEAnt** OTFT at different gate voltages (V_g).

than the second transition temperature on the DSC curve, device performance started to degrade and a lower field effect mobility of 1.0×10^{-3} cm^2/Vs was obtained.

On the other hand, the longer alkyl chain of **DDPEAnt** could have hindered the formation of a crystalline structure, and so led to a mobility half the value of **DHPEAnt** (2.0×10^{-3} cm^2/Vs). The output characteristics along with plots of the drain current (I_d) versus gate voltage (V_g) of the relevant device are shown in Figure 6. In addition, no further thermal annealing increased device performance, presumably due to

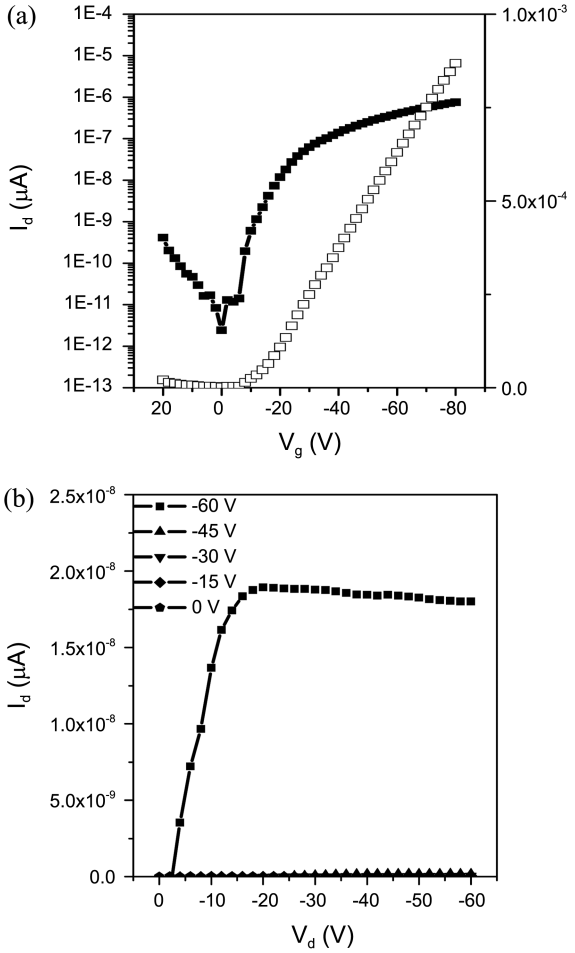

Figure 7. (a) Drain current (I_d) versus gate voltage (V_g) characteristics of **DHPEAnt**. (b) Drain current (I_d) versus drain-source voltage (V_d) characteristics of the **DHPEAnt** OTFT at different gate voltages (V_g).

the degradation of the **DDPEAnt** film. In sum, two anthracene derivatives were thought to exhibit better device performance when they formed a more complete semiconducting film. The relatively low solubility of these two materials is considered a weakness in their application to TFT. In case of **DDPEXAnt**, due to its high crystallinity and low solubility could not be applied to the solution process.

Conclusions

We synthesized novel 4-alkylethynylbenzene end-capped oligomers from a Sonogashira coupling reaction of anthracene with **5a-c** and investigated their properties. Investigation of their thermal properties revealed that all oligomers had good thermal stability (between 417 °C and 458 °C). Investigation of the optical and electrochemical properties showed that the synthesized oligomers have higher oxidation potentials due to their high HOMO energy levels (−5.39 eV for **DHPEAnt**, −5.38 eV for **DDPEAnt** and −5.43 eV for **DDPEXAnt**). Thin films of **DHPEAnt** and **DDPEAnt** deposited by spin coating resulted in OTFTs which showed hole field-effect mobilities of 2.0×10^{-3} cm^2/Vs. Only slight-

ly better mobilities (4.0×10^{-3} cm^2/Vs) were obtained by a 160 °C thermal annealing process of the active layer onto Si/SiO_2.

Experimental Section

Materials and Measurements.

Materials: 2-Bromobenzene, decanoyl chloride, hexanoyl chloride, aluminum chloride, hydrazine hydrate, trimethylsilylacetylene, diisopropylamine, tetrabutylammonium fluoride and [1,1'-bis(diphenylphosphino)ferrocene]dichloropalladium (II) were purchased from Aldrich Chemical Co. 4-Bromophenol, triethylene glycol, copper iodide and triphenyl phospine were purchased from TCI. All reagents purchased commercially were used without further purification except for diethylether and tetrahydrofuran (THF) dried with sodium/benzophenone. Synthesis of 2,9-dibromoanthracene was carried out according to literature procedures.[13]

Measurements: A Shimadzu FT-IR spectrometer was used to recorded IR spectra. ^{1}H-NMR and ^{13}C-NMR spectra were recorded with Avance 300 and DRX 500 MHz NMR Bruker spectrometers, and chemical shifts were reported in ppm units with tetramethylsilane as the internal standard. Thermal gravimetric analysis (TGA) was performed under nitrogen on a TA Instruments 2050 thermal gravimetric analyzer. Samples were heated using a 10 °C/min heating rate from 50 °C to 800 °C. Differential scanning calorimetry (DSC) was conducted under nitrogen on a TA Instruments 2100 differential scanning calorimeter. Samples were heated at 10 °C/min from 50 °C to 300 °C. Mass spectra were measured by a Jeol JMS-700 mass spectrometer. UV-vis absorption and photoluminescence (PL) spectra were measured with a Perkin Elmer LAMBDA-900 UV/VIS/NIR spectrophotometer and a LS-50B luminescence spectrophotometer, respectively. Cyclic voltammograms of the oligomers were recorded on an Epsilon E3 at a room temperature in a 0.1 M solution of tetrabutylammonium perchlorate (Bu_4NClO_4) in $CHCl_3$ under nitrogen gas protection at a scan rate of 50 mV/s. A Pt wire and a $Ag/AgNO_3$ electrode were used as the counter and reference electrodes, respectively.

Synthetic Procedures.

4-Bromohexanoylbenzene (1a): Hexanoyl chloride (120 g, 0.89 mol) was added dropwise to a mixture of bromobenzene (279 g, 1.78 mol) and aluminum chloride (143 g, 1.07 mol). The reaction mixture was stirred at 50 °C for 1 h. The reaction mixture was cooled to room temperature and poured into ice water. It was then extracted with methylene chloride. The organic phase was washed with dilute acid (2 M HCl) and water, dried over anhydrous magnesium sulfate. The solvent was removed by rotary evaporator and the residue was purified by recrystallization with ethanol to afford **1a** (110 g, 48%) as white plates, mp 59-60 °C. ^{1}H NMR (300 MHz, $CDCl_3$): δ 7.81 (d, 2 H, J = 8.61 Hz), 7.58 (d, 2 H, J = 8.60 Hz), 2.93 (t, 2 H, J = 7.36 Hz), 1.76-1.66 (m, 2 H), 1.36-1.34 (m, 4 H), 0.92 (t, 3 H, J = 6.81 Hz). ^{13}C NMR (75 MHz, $CDCl_3$): δ 199.3, 135.8, 131.8, 129.6, 127.9, 38.5, 31.5, 23.9, 22.5, 13.9. IR (KBr) ν [cm^{-1}]: 2960, 2918, 2850, 1600, 1510. MS (EI): *m/z* 254 (M+).

4-Bromodecanoylbenzene (1b): Following the procedure for compound **1a**, compound **1b** was prepared using decanoyl chloride (46.7 g, 0.245 mol), bromobenzene (77 g, 0.49 mol), and aluminum chloride (39.7 g, 0.294 mol), respectively. The residue was purified by recrystallization with ethanol to afford **1b** (79.38 g, 65%) as white plates. mp 64 °C. ^{1}H NMR (300 MHz, $CDCl_3$): δ 7.84 (d, 2 H, J = 8.42 Hz), 7.61 (d, 2 H, J = 8.37 Hz), 2.93 (t, 2 H, J = 7.38 Hz), 1.77-1.68 (m, 2 H), 1.28 (m, 12 H), 0.89 (t, 3 H, J = 6.55 Hz). ^{13}C NMR (75 MHz, $CDCl_3$): δ 199.4, 135.8, 131.8, 129.6, 128.0, 38.6, 31.9, 29.5, 29.3, 29.2, 24.3, 22.7, 14.1. IR (KBr) ν [cm^{-1}]: 2954, 2915, 2847, 1584, 1471. MS (EI): *m/z* 310 (M+).

4-Bromohexylbenzene (2a): A mixture of **1a** (101 g, 0.396 mol), hydrazine hydrate (45 mL), and KOH (88.9 g, 1.584 mol) in triethylene glycol (500 mL) was deionized at atmospheric pressure until the temperature of the reaction mixture reached 210 °C. After cooling down to room temperature, the resulting mixture was poured into water, acidified with conc HCl solution, and extracted with methylene chloride. The organic phase was washed with water and dried over anhydrous magnesium sulfate. The solvent was removed by rotary evaporator and the residue was purified by flash silica gel chromatography with hexane to afford **2a** (57 g, 48%) as a colorless oil. ^{1}H NMR (300 MHz, $CDCl_3$): δ 7.45 (d, 2 H, J = 8.33 Hz), 7.11 (d, 2 H, J = 8.32 Hz), 2.63 (t, 2 H, J = 7.69 Hz), 1.67-1.62 (m, 2 H), 1.40-1.35 (m, 6 H), 0.97 (t, 3 H, J = 6.60 Hz). ^{13}C NMR (75 MHz, $CDCl_3$): δ 140.9, 132.3, 129.2, 120.3, 35.5, 32.4, 31.9, 27.5, 23.3, 14.0. IR (KBr) ν [cm^{-1}]: 2930, 2917, 2855, 1490. MS (EI): *m/z* 240 (M+).

4-Bromodecylbenzene (2b): Following the procedure for compound **2a**, compound **2b** was prepared using **1b** (159 g, 051 mol), hydrazine hydrate (70 mL), and KOH (114.46 g, 2.04 mol) in triethylene glycol (700 mL). The residue was purified by recrystallization with ethanol to afford **2b** (86 g, 59%) as a colorless oil. ^{1}H-NMR (300 MHz, $CDCl_3$): δ 7.43 (d, 2 H, J = 8.18 Hz), 7.09 (d, 2 H, J = 8.21 Hz), 2.58 (t, 2 H, J = 6.8 Hz), 1.64-1.58 (m, 2 H), 1.30 (m, 21 H), 0.92 (t, 3 H, J = 6.57 Hz). ^{13}C-NMR (75 MHz, $CDCl_3$): δ 141.9, 131.3, 130.2, 119.3, 35.4, 31.9, 31.4, 29.6 (2 peaks), 29.5, 29.4, 29.2, 22.7, 14.1. IR (KBr) ν [cm^{-1}]: 2960, 2900, 2869, 1487. MS (EI): *m/z* 296 (M+).

1-Bromo-4-(decyloxy)benzene (3): 4-Bromophenol (5 g, 28.9 mmol), bromodecane (7.06 g, 6.6 mL, 31.79 mmol), NaI (0.3 g, 2.02 mmol) and KOH (1.78 g, 31.79 mmol) were dissolved in ethanol (50 mL). The mixture was stirred for 27 h to reflux. After cooling down to room temperature, the solvent was removed by rotary evaporator. The resulting mixture was poured into water and extracted with ethyl acetate. The organic phase was washed with water and dried over anhydrous magnesium sulfate. The solvent was removed by rotary evaporator and the residue was purified by flash silica gel chromatography with hexane to afford **3** (8.9 g, 98%) as a colorless oil. ^{1}H-NMR (300 MHz, $CDCl_3$): δ 7.40 (d, 2 H, J = 8.81 Hz), 6.81 (d, 2 H, J = 8.84 Hz), 3.93 (t, 2 H,

J = 6.55 Hz), 1.82-1.77 (m, 2 H), 1.31 (m, 14 H), 0.92 (t, 3 H, *J* = 6.52 Hz). ^{13}C-NMR (75 MHz, $CDCl_3$): δ 158.3, 132.2, 116.3, 112.6, 68.3, 31.9, 29.6, 29.4, 29.3, 29.2. 26.0, 22.7, 14.1. IR (KBr) ν [cm^{-1}]: 2925, 2853, 1489. MS (EI): *m/z* 312 (M+).

(2-(4-Hexylphenyl)ethynyl)trimethylsilane (4a): 2a (20 g, 82.93 mmol), trimethylsilylacetylene (11.5 mL, 82.93 mmol), Pd(dppf)Cl_2 (1.3 g, 1.66 mmol), CuI (0.95 g, 4.98 mmol), PPh_3 (0.44 g, 1.66 mmol), and diisopropylamine (200 mL) were charged sequentially into a two-neck flask under nitrogen and heated to reflux for 16 h. The volatile compounds were removed under vacuum, and the resulting solid was extracted into diethyl ether. The organic extract was washed brine solution and dried over anhydrous magnesium sulfate. The solvent was removed by rotary evaporator and the residue was purified by silica gel chromatography with hexane to afford **4a** (16.7 g, 78%) as a colorless oil. ^{1}H-NMR (300 MHz, $CDCl_3$): δ 7.51 (d, 2 H, *J* = 8.18 Hz), 7.20 (d, 2 H, *J* = 8.14 Hz), 2.68 (t, 2 H, *J* = 7.69 Hz), 1.69-1.66 (m, 2 H), 1.14 (m, 6H), 1.00 (t, 3 H, *J* = 6.77 Hz), 0.38 (s, 9 H). ^{13}C-NMR (75 MHz, $CDCl_3$): δ 143.6, 132.0, 128.5, 128.4, 128.3, 120.5, 105.6, 93.2, 36.0, 31.8, 31.3, 29.0, 22.7, 14.2, 13.9. IR (KBr) ν [cm^{-1}]: 2957, 2929, 2857, 1507, 1455. MS (EI): *m/z* 258 (M+).

(2-(4-Decylphenyl)ethynyl)trimethylsilane (4b): Following the procedure for compound **4a**, compound **4b** was prepared using **2b** (10 g, 33.41 mol), trimethylsilylacetylene (4.6 mL, 33.41 mol), Pd(dppf)Cl_2 (0.54 g, 0.66 mmol), CuI (0.38 g, 2.00mmol), PPh_3 (0.17 g, 0.66 mmol) and diisopropylamine (50 mL). The residue was purified by silica gel chromatography with hexane to afford **4b** (9.3 g, 88%) as a colorless oil. ^{1}H-NMR (300 MHz, $CDCl_3$): δ 7.52 (dd, 2 H, *J* = 8.17 Hz, *J* = 8.53 Hz), 7.21 (dd, 2 H, *J* = 7.98 Hz, *J* = 8.20 Hz), 2.72-2.62 (m, 2 H), 1.69 (m, 2 H), 1.90 (s, 9 H), 1.27-1.22 (m, 14 H), 1.01 (t, 3 H, *J* = 6.53). ^{13}C-NMR (75 MHz, $CDCl_3$): δ 143.5, 141.8, 132.0, 131.3, 130.2, 128.3, 120.9, 107.6, 89.4, 36.0, 35.5, 32.1, 32.0, 29.6, 29.5, 22.8, 18.8, 18.7, 14.2, 11.5. IR (KBr) ν [cm^{-1}]: 2957, 2926, 2855, 1506, 1456. MS (EI): *m/z* 314 (M+).

(2-(4-Decyloxyphenyl)ethynyl)trimethylsilane (4c): Following the procedure for compound **4a**, compound **4c** was prepared using **3** (7 g, 22.34 mmol), trimethylsilylacetylene (3.4 mL, 24.57 mmol), Pd(dppf)Cl_2 (0.37 g, 0.45 mmol), CuI (0.25 g, 1.34mmol), PPh_3 (0.12 g, 0.45 mmol) and diisopropylamine (50 mL). The residue was purified by silica gel chromatography with hexane to afford **4c** (4 g, 54%) as a colorless oil. ^{1}H-NMR (300 MHz, $CDCl_3$): δ 7.43 (d, 2 H, *J* = 8.84 Hz), 6.84 (d, 2 H, *J* = 8.86 Hz), 3.96 (t, 2 H, *J* = 6.58 Hz), 1.81-1.74 (m, 2 H), 1.30 (m, 14 H), 0.91 (t, 3 H, *J* = 6.70 Hz), 0.26 (s, 9 H). ^{13}C-NMR (75 MHz, $CDCl_3$): δ 159.3, 133.4, 115.0, 114.3, 105.3, 92.3, 68.0, 31.9, 29.6, 29.4, 29.3, 29.2, 26.0, 22.7, 14.1. IR (KBr) ν [cm^{-1}]: 2922, 2855, 1506, 1469. MS (EI): *m/z* 330 (M+).

1-Ethynyl-4-hexylbenzene (5a): A 1 M solution of tetrabutylammonium fluoride in THF (22.1 mL, 22.1 mmol) was added to a solution of **4a** (16.8 g, 65 mmol) in THF (100 mL), and the resulting solution was stirred under nitrogen at room temperature for 2 h. The solvent was evaporated by adding silica gel (20 g) to afford a plug, which in turn was purified by silica gel chromatography with hexane to afford 5**a** (5.1 g, 42%) as a colorless oil. ^{1}H-NMR (300 MHz, $CDCl_3$): δ 7.47 (d, 2 H, *J* = 8.11 Hz), 7.19 (d, 2 H, *J* = 8.02 Hz), 3.07 (s, 1 H), 2.64 (t, 2 H, *J* = 7.68 Hz), 1.66-1.57 (m, 2 H), 1.34 (m, 6 H), 0.93 (t, 3 H, *J* = 6.34 Hz). ^{13}C-NMR (75 MHz, $CDCl_3$): δ 143, 132.1, 128.4, 119.3, 83.9, 76.5, 35.9, 31.7, 31.2, 29.0, 22.6, 14.3. IR (KBr) ν [cm^{-1}]: 2956, 2927, 2857, 1508, 1458. MS (EI): *m/z* 186 (M+).

1-Decyl-4-ethynylbenzene (5b): Following the procedure for compound **5a**, compound **5b** was prepared using **4b** (9.3 g, 29.56 mol), a 1 M solution of tetrabutylammonium fluoride in THF (10 mL, 10.05 mmol) and THF (70 mL). The residue was purified by silica gel chromatography with hexane to afford **5b** (5 g, 70%) as a colorless oil. ^{1}H-NMR (300 MHz, $CDCl_3$): δ 7.47 (d, 2 H, *J* = 7.89 Hz), 7.19 (d, 2 H, *J* = 7.91 Hz), 3.08 (s, 1 H), 2.65 (t, 2 H, *J* = 7.70 Hz), 1.69-1.63 (m, 2 H), 1.35 (m, 14 H), 0.95 (t, 3 H, *J* = 6.47 Hz). ^{13}C-NMR (75 MHz, $CDCl_3$): δ 144.0, 132.1, 128.4, 119.3, 83.9, 76.5, 36.0, 32.0, 31.9, 31.3, 29.6, 29.5, 29.4, 29.3, 22.7, 14.2. IR (KBr) ν [cm^{-1}]: 2927, 2855, 1367. MS (EI): *m/z* 242 (M+).

1-(Decyloxy)-4-ethynylbenzene (5c): Following the procedure for compound **5a**, compound **5c** was prepared using **4c** (2.1 g, 6.35 mmol), a 1 M solution of tetrabutylammonium fluoride in THF (2.16 mL, 2.16 mmol), and THF (20 mL). The residue was purified by silica gel chromatography with hexane to afford **5c** (1.1 g, 67%) as a colorless oil. ^{1}H-NMR (300 MHz, $CDCl_3$): δ 7.47 (d, 2 H, *J* = 8.79 Hz), 6.87 (d, 2 H, *J* = 8.81 Hz), 3.97 (t, 2 H, *J* = 6.55 Hz), 1.81 (m, 2 H), 1.32 (m, 14 H), 0.93 (t, 3 H, *J* = 6.95 Hz). ^{13}C-NMR (75 MHz, $CDCl_3$): δ 159.5, 133.5, 114.4, 113.9, 83.8, 75.6, 68.0, 32.0, 31.7, 29.6, 29.4 (two peak), 29.2, 26.1, 22.7, 14.1. MS (EI): *m/z* 258 (M+).

2,6-Bis[2-(4-hexylphenyl)ethynyl]anthracene (DHPEAnt): 2,6-Dibromoanthracene (1 g, 2.98 mmol), **5a** (1.22 g, 0.56 mmol), Pd(dppf)Cl_2 (0.13 g, 0.15 mmol), CuI (58 mg, 0.3 mmol), and diisopropyl amine/toluene (20 mL/20 mL) were charged sequentially into a two-neck flask under nitrogen and heated to reflux for 16 h. The volatile compounds were removed under vacuum and the resulting solid was extracted into diethyl ether. The extract was separated to solution phase and precipitate. The precipitate was washed with diethyl ether, the solution phase was washed with brine solution and dried over anhydrous magnesium sulfate. The solvent was removed by rotary evaporator and the residue was purified by silica gel chromatography with hexane to afford **DHPEAnt** (0.81 g, 50%) as a pale yellow solid. mp 217 °C. ^{1}H NMR (300 MHz, $CDCl_3$): δ 8.37 (s, 2H), 8.21 (s, 2H), 7.99 (d, 2H, *J* = 8.64 Hz), 7.57 (d, 2H, *J* = 8.66 Hz), 7.54 (d, 4H, *J* = 7.62 Hz), 7.28 (d, 4H, *J* = 7.44 Hz), 2.65 (t, 4H, *J* = 7.13 Hz), 1.65 (m, 4H), 1.34 (m, 12H), 0.91 (m, 6H). ^{13}C NMR (75 MHz, $CDCl_3$): δ 143.7, 131.6, 131.1, 128.5, 128.3, 128.1, 126.2, 120.7, 120.3, 90.9. 77.2, 36.0, 31.7, 31.2, 28.9, 22.6, 14.1. IR (KBr) ν [cm^{-1}]: 2956, 2917, 2848, 1566, 1480. MS (EI): *m/z* 546 (M+).

2,6-Bis[2-(4-decylphenyl)ethynyl]anthracene (DDPEAnt):

Following the procedure for **DHPEAnt**, **DDPEAnt** was prepared using 2,6-dibromoanthracene(1 g, 2.98 mmol), **5b** (1.44 g, 5396 mmol), Pd(dppf)Cl_2 (49 mg, 0.06 mmol), CuI (34 mg, 0.18 mmol), PPh_3 (16 mg, 0.06 mmol), and diisopropylamine (15 mL). The residue was purified by silica gel chromatography with hexane to afford **DDPEAnt** (0.75 g, 38%) as a pale yellowish green solid. mp 204 °C. ^{1}H NMR (300 MHz, $CDCl_3$): δ 8.36 (s, 2H), 8.21 (s, 2H), 7.99 (d, 2H, J = 8.81 Hz), 7.58 (d, 2H, J = 8.57 Hz), 7.54 (d, 4H, J = 8.07 Hz), 7.23 (d, 4H, J = 8.16 Hz), 2.66 (t, 4H, J = 7.68 Hz), 1.68-1.61 (m, 4H), 1.34-1.30 (m, 28H), 0.91 (t, 6H, J = 6.71 Hz). ^{13}C NMR (75 MHz, $CDCl_3$): δ 143.7, 131.6, 131.0, 128.6, 128.3, 128.1, 126.2, 120.7, 120.3, 91.0. 89.4, 36.0, 31.9, 31.3, 29.6, 29.5, 29.3, 22.7, 14.1. IR (KBr) ν [cm^{-1}]: 2956, 2917, 2848, 1511, 1467. MS (EI): *m/z* 658 (M+).

2,6-Bis[2-(4-decyloxyphenyl)ethynyl]anthracene (DDPEXAnt): Following the procedure for **DHPEAnt**, **DDPEXAnt** was prepared using 2,6-dibromoanthracene (0.72 g, 2.13 mmol), **5c** (1.1 g, 4.26 mmol), Pd(dppf)Cl_2 (90 mg, 0.11 mmol), CuI (40 mg, 0.21 mmol), and triethylamine/toluene (15 mL/15 mL). The residue was purified by silica gel chromatography with hexane to afford **DDPEXAnt** (0.4 g, 27%) as a pale yellowish green solid. mp 220 °C. ^{1}H NMR (300 MHz, $CDCl_3$): δ 8.37 (s, 2H), 8.18 (s, 2H), 7.99 (d, 2H, J = 8.81 Hz), 7.58-7.57 (m, 6H), 6.93 (d, 4H, J = 9.00 Hz), 4.01 (t, 4H, J = 7.68 Hz), 1.87-1.77 (m, 4H), 1.32 (m, 28H), 0.91 (t, 6H, J = 6.71 Hz). IR (KBr) ν [cm^{-1}]: 2954, 2919, 2850, 1602, 1510. MS (EI): *m/z* 691 (M+).

Device Fabrication. To determine the device performance for each material, we employed bottom-gate top-contact geometry. We used a heavily N-doped silicon substrate and thermally deposited SiO_2 (300 nm) as the dielectric layer. Various surface modifications of the cleaned SiO_2 substrate were performed to change its surface characteristics. Generally, a more effective charge carrier transfer is achieved with more hydrophobic surfaces. Therefore, hydrophobic surface treatments of the dielectric surface such as with hexamethyldisilazane (HMDS), octadecyltrichlorosilane (OTS-18), and polydimethylsiloxane (PDMS), were performed *via* the well-known solution method. The water contact angles for each case were measured to 25 ± 2° (untreated), 68 ± 2° (HMDS), 99 ± 2° (OTS-8), 108 ± 1° (OTS-18), 109 ± 2° (PDMS). Semiconducting materials were usually deposited onto each modified dielectric surface *via* spin-casting, drop-casting with chloroform, toluene, and chlorobenzene as solvents, and in some cases substrate heating to fabricate a more uniform layer. The Au source and drain electrode were thermally evaporated onto the semiconducting layer at a thickness of 100 nm, and a shadow mask was used to make the patterns and a channel region 1500 μm long and 150 μm wide. The field effect mobility was extracted from the saturation regime for transfer characteristics, using the equation $\mu_{sat}=(2I_{DS}L)/(WC(V_g-V_{th})^2)$, where I_{DS} is the saturation drain current, C is the capacitance of the oxide dielectric, V_g is the gate bias, and V_{th} is the threshold voltage.

Acknowledgments. This research was supported by the Brain Korean Program 21 (BK21), a grant (F0004010-2011-34) from Information Display R&D Center, one of the Knowledge Economy Frontier R&D Program funded by the Ministry of Knowledge Economy of Korean government, and Basic Science Research Program through the National Research Foundation of Korea (NRF) funded by the ministry of Education, Science and Technology (Grant Number: 2010-0023775)

Reference and Notes

1. Jun-ichi, N.; Shigeki, M.; Hirokazu, T.; Yoshiro, Y. *Chem. Lett*. **2006**, *35*, 1236.
2. Kimberly, C. D.; John, E. A.; Yueh-Lin, L. *Adv. Mater*. **2006**, *18*, 1721.
3. (a) Pope, M.; Swenberg, C. E. *Electronic Processes in Organic Crystals and Polymers*; Oxford University Press: New York, 1999. (b) Karl, N.; Marktanner, J. Mol. *Cryst. Liq. Cryst*. **2001**, *355*, 149.
4. Dimitrakopoulos, C. D.; Malenfant, P. R. L. *Adv. Mater*. **2002**, *14*, 99.
5. (a) Katz, H. E.; Bao, Z.; Gilat Acc, S. L. *Chem. Res*. **2001**, *34*, 359. (b) Garnier, F.; Yassar, A.; Hajlaoui, R.; Horowitz, G.; Deloffre, F.; Servet, B.; Ries, S.; Alnot, P. *J. Am. Chem. Soc*. **1993**, *115*, 8716.
6. Gundlach, D. J.; Lin,Y.; Jackson, T. N.; Schlom, D. G. *Appl. Phys. Lett*. **1997**, *71*, 3853.
7. Ito, K.; Suzuki, T.; Sakamoto, Y.; Kubota, D.; Inoue, Y.; Sato, F.; Tokito, S. *Angew. Chem., Int. Ed*. **2003**, *42*, 1159.
8. Meng, H.; Zheng, J.; Lovinger, A. J.; Wang, B.; Van Patten, P. G.; Bao, Z. *Chem. Mater*. **2003**, *15*, 1778.
9. Meng, H.; Sun, F.; Goldfinger, M. B.; Jaycox, G. D.; Li, Z.; Marshall, W. J.; Blackman, G. S. *J. Am. Chem. Soc.* **2005**, *127*, 2406.
10. Zhao, Q.; Kim, T. H.; Park, J. W.; Kim, S. O.; Jung, S. O.; Kim, J. W.; Ahn, T.; Kim, Y. H.; Yi, M. H.; Kwon, S. K. *Adv. Mater*. **2008**, *20*, 4868.
11. Garnier, F.; Yassar, A.; Hajlaoui, R.; Horowitz, G.; Deloffre, F.; Servet, B.; Ries, S.; Alnot, P. *J. Am. Chem. Soc*. **1993**, *115*, 8716.
12. Ponomarenko, S. A.; Kirchmeyer, S.; Elschner, A.; Alpatova, N. M.; Halik, M.; Klauk, H.; Zschieschang, U.; Schmid, G. *Chem. Mater*. **2006**, *18*, 579.
13. Lee, S. K.; Yang, W. J.; Choi, J. J.; Kim, C. H.; Jeon, S. J.; Cho, B. R. *Org. Lett.* **2005**, *7*, 323.
14. Boudreault, P. L. T.; Virkar, A. A.; Bao, Z.; Leclerc, M. *Org. Electron*. **2010**, *11*, 1649.
15. Kim, H. S.; Kim, Y. H.; Kim, T. H.; Noh, Y. Y.; Pyo, S. M.; Yi, M. H.; Kim, D. Y.; Kwon, S. K. *Chem. Mater*. **2007**, *19*, 3561.
16. Miura, Z.; Chen, H.; Ujii, S.; De Feyter, M.; Zdanowska, P.; Jonkheijm, A. P. H. J.; chen ning, E.W.; Meijer, F. W.; Schryver, F. C. D. *J. Am. Chem. Soc*. **2003**, *125*, 14968.
17. Ando, S.; Nishida, J.; Fujiwara, E.; Tada, H.; Inoue, Y.; Tokito, S.; Yamashita, Y. *Chem. Mater*. **2005**, *17*, 1261.